Conference Proceedings

Solar World Congress 2015
Daegu, Korea, 08 – 12 November 2015

Design for a Solar Thermal Energy Storage System

Ramón Gutiérrez Razo[1], Bruno Cárdenas Castañeda[1], Noel Leon Rovira[1]

Tecnológico de Monterrey - Centro de Innovación en Diseño y Tecnología, Monterrey, Nuevo León, México

Abstract

The design of a Thermal Energy Storage unit (TES) is shown to use solar energy at times where there is intermittent, shortage or lack of solar radiation. The TES unit is made of five parts: heat reservoir, heat reservoir container, heat receptor – transmitter system, thermal insulator and structural support. The TES unit material's must be abundant, be of common usage in industry, obtained either from recycling or industrial wastes. Also the materials must be non – toxic and non – flammable. Three TES designs will be shown pointing out the opportunity areas found in each one in order to achieve a TES unit with the best performance possible.

Keywords: *Solar energy, Latent heat, glass, TES*

1. Introduction

Fossil fuels domain the market to cover the world's ever growing energy demands [1]. However the extended use of fossil fuels involve environmental consequences, can cause disturbances in the global economy to sudden shortage or surplus of fossil fuels, and at one time these kind of fuels will end. Renewable energies can be a solution to the dependency of fossil fuels. Renewable energies are at the time in development, the initial investment can be high and use to be intermittent.

Currently there are solar concentration systems such as solar power towers and parabolic trough for storing heat in molten salts. However these systems require large areas of land for installation and complex piping and pumping system to withstand temperatures from 300°C to 500°C besides the corrosion caused by the salts. Both systems also require an active tracking of the sun throughout the day which increases the cost and complexity of the system [2, 3].

Solar energy has the characteristic of being abundant and clean, however the development of technologies that exploit this resource have high investments and are still under development. A disadvantage of solar energy is to be intermittent, available only in daylight and depend to weather conditions. In order to solve the aforementioned problem TES units have been developed so that solar energy can be used during periods when solar radiation is not favorable or not present.

Research of a concept of electric and mechanical energy generation has been made by the usage of stored thermal energy from the concentration of solar radiation. The search of material of common usage in industry, recyclable, or from industrial waste has been priority in the design of TES units in order to reduce costs and promote the use of solar energy.

The TES unit requires materials with good thermal conductivity, high energy density per unit of volume and mass for the heat reservoir; in the zone where energy is inserted and extracted the materials require high temperature resistance and good thermal conductivity, besides good solar radiation absorptance for the energy receptor zone; for the materials to be used as heat reservoir container and thermal insulator in order to decrease the reservoir container temperature as close to room temperature requires low thermal conductivity and high temperature resistance.

All material must be non-toxic, and non – auto ignitable at the working temperature of the TES unit.

As a first approach the research aspire to design a TES unit to supply 20 kWh of electric energy. This electricity consume is the average consume of each domestic user in Mexico.

doi:10.18086/swc.2015.02.07 Available at http://proceedings.ises.org

2. Experiment

For the development of the TES unit finite element method simulations by computer and experimental tests have been made. The finite element method takes into account the variation of the thermal conductivity and specific heat values according to changes in the temperature of the material. Three different designs of TES units will be shown pointing out the most relevant results and the opportunity areas found.

The three TES units have in common the usage of soda lime glass as a heat reservoir obtained from wastes; all the TES units use graphite obtained from industrial wastes as the energy reception – extraction system; the three heat reservoir containers are made of alumina; the thermal insulator in the three units is made of ceramic fiber and the external container is made of steel A – 36. The last three aforementioned materials are of common usage in the industry and of lower cost compared with other options.

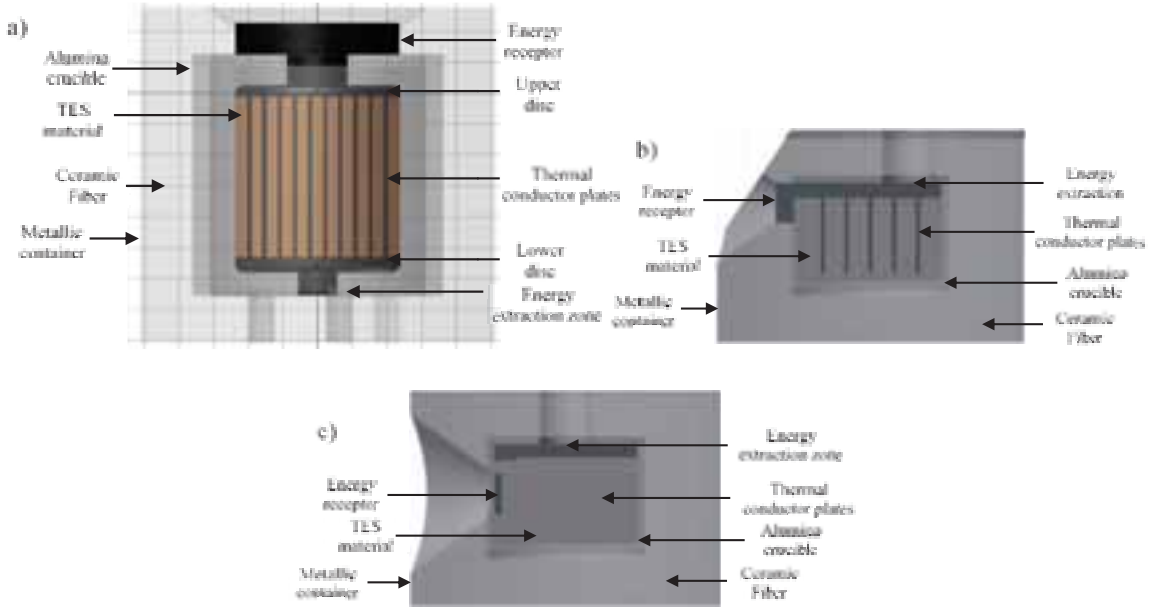

Fig. 1: TES designs. Each grid represent 4inches (around 10 cm.) The three TES drawings are at the same scale for comparative reasons.

Soda lime glass selection as a heat reservoir was based on having a good heat capacity per unit of mass. Graphite was chosen as a thermal receiver - transmitter based on its working temperature which is around 2500°C and 3000°C whenever it is protected from an oxidizing atmosphere [4], and having a good heat conductivity. Both materials share the characteristic of being abundant, and can be obtained from waste or recycled materials.
The A TES design was built and experimental tests were run. With the results obtained in the design A designs B and C were made in order to solve the shortcomings in the performance of this first design. Finite element method analysis of the TES units B and C were made in order to show the improvement in latter TES design compared with previous ones.
Designs B and C were made with 62% and 55% of the heat reservoir mass of the Design A respectively with the intention of get experimental test quicker. Designs B and C have in common the diminishing in weight and number of components of graphite and have the energy receptor as close as possible to the heat reservoir.

Tab. 1: Volume and mass of the heat reservoir of the TES units

Heat Reservoir	Volume [m³]	Mass [Kg]
Design A	0.06949	173.725
Design B	0.04303	107.575
Design C	0.0385	96.25

In the design B the thermal conductor plates made of graphite are at 90° of the direction of the incoming heat flux from the energy receptor, in the design C these plate are in the same direction of the incoming heat flux. In the

design B the energy receptor is in the upper part of the TES unit and connected to the heat reservoir by an area equivalent to the third part of the energy spot, in the design C the energy receptor is at the middle of the TES unit and is slightly inside of the heat reservoir container connected to a graphite plate non – existent in the design B.

The TES unit is designed to be connected to a Stirling Engine with a capacity of 1 kW and with a thermal efficiency of 0.25. The Stirling Engine needs a temperature of 500°C or more to operate.

For the computer simulation the Autodesk Simulation Mechanical 2014 software was used.

The following mathematical models were used to take into account the changes in the specific heat and thermal conductivity values as the temperature fluctuates.

$$C_p = 2.268 - 10.153 \times 10^{-6}T - 377.70014T^{-1} - 181791.8712T^{-2} + 6.66548856 \times 10^{7}T^{-3} - 6.011905920 \times 10^{9}T^{-4} \left[\frac{J}{g-K}\right] \quad \text{(eq. 1)}$$

$$k = \frac{418.4}{2.4 + 3.46 \times 10^{-3}T + 8.5 \times 10^{11}e^{-8.9\times10^{4}/T}} \left[\frac{w}{m-K}\right] \quad \text{(eq. 2)}$$

$$C_p = 9.474 \times 10^{-15}T^{5} - 3.923 \times 10^{-11}T^{4} + 6.221 \times 10^{-8}T^{3} - 4.746 \times 10^{-5}T^{2} + 1.814 \times 10^{-2}T - 1.833 \left[\frac{J}{g-K}\right] \quad \text{(eq. 3)}$$

$$k = -1.413 \times 10^{-14}T^{5} + 6.083 \times 10^{-11}T^{4} - 3.120 \times 10^{-8}T^{3} - 2.853 \times 10^{-5}T^{2} + 2.512 \times 10^{-2}T - 3.668 \left[\frac{w}{m-K}\right] \quad \text{(eq. 4)}$$

The specific heat of the graphite model was obtained by the fitting of two mathematical models [1]. The specific heat graphite model is useful in the range of 200K to 1000K, however the model can be expanded to temperatures of 3270K where the specific heat value almost stabilize (Eq. 1). For the thermal conductivity graphite model it was used a mathematical model made by N.S. Rasor and J.D. McClelland [8] and is useful in the range of 300K to 3270K (Eq. 2). It is assumed that the graphite used is of commercial grade quality and with isotropic properties.

The soda – lime glass store thermal energy as sensible heat. In the industry of soda – lime glass it is considered a value of 2550 kJ to bring 1 kg of soda lime glass to a working temperature [9]. The specific heat of the soda – lime glass model shown in the following section is useful in the range of 270K and 1350K (Eq. 3) [1] for higher temperature values a constant soda lime glass Cp of 1.4 kJ/kg-°C was used in the simulation. The thermal conductivity of soda lime glass model was created by the fitting of three mathematical models (Eq. 4) [1], this model is useful in the range of 270K to 1580K, for higher temperature values a constant soda lime glass thermal conductivity value of 82.4 w/m-°C was used in the simulation [6]. In the figures 2 and 3 are shown the values of the specific heat and thermal conductivity values respectively. More information about the values taken into account in the simulation for the refractory concrete, ceramic fiber and A-36 steel can be found in [6] and [13].

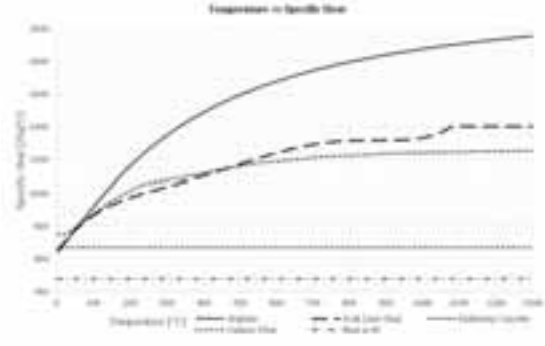

Fig. 2: Temperature vs Specific Heat

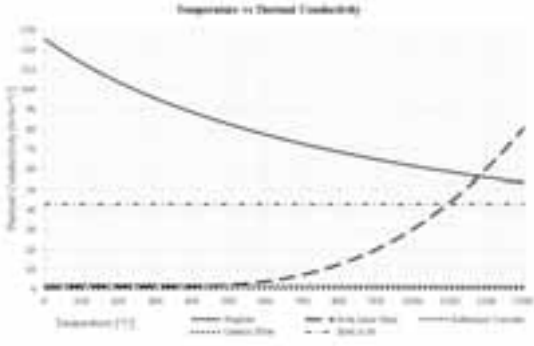

Fig. 3: Temperature vs Thermal Conductivity

Tab. 2: Material density values

Material	Density [Kg/m³]	Reference
Graphite	1700	[1]
Soda Lime Glass	2500	[1]
Refractory	2630	[10,11]
Ceramic Fiber	96	[12]
Steel A - 36	7850	[13]

A finite element method of the design B and C was made for 10 days of operation. Each TES unit will receive 5.625 kW at the energy receptor zone daily by 8 hours receiving a total of 45.0 kWh (Charge cycle) followed by 16 hours of zero entry and extraction energy (Rest cycle). The energy receptor spot had a value of emissivity of 0.95 during the charging periods and a value of zero during the rest of the day. A convection coefficient of 3.22 w/°C-m² was used over the exterior of the TES unit. At days 9 and 10 an extraction of 4.0 kW of heat over the extraction zone was applied. (Heat extraction cycle).

The central point of the energy receptor and extraction zone was taken in the finite element method simulations of the designs B and C and was assumed that the whole zone had a similar temperature. Using the Stephan Boltzmann Black Radiation (Eq. 5) [14] model for black body at the energy receptor zone was possible to calculate and estimate for the radiation heat losses. Checking at the time that the energy extraction point was above 500°C was possible to estimate how much energy was extracted by the Stirling engine.

$$Q_{RadLosses} = \varepsilon\sigma A(T_S^4 - T_{Amb}^4) \qquad \text{(eq. 5)}$$

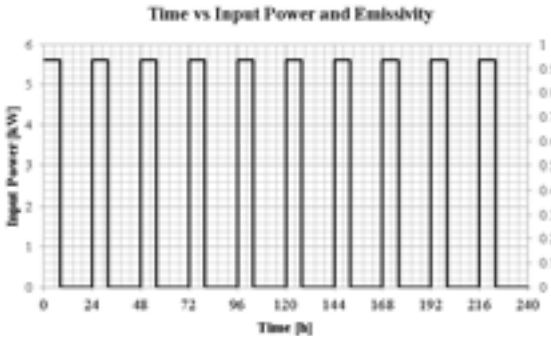

Fig. 4: Time vs Input Power and Emissivity

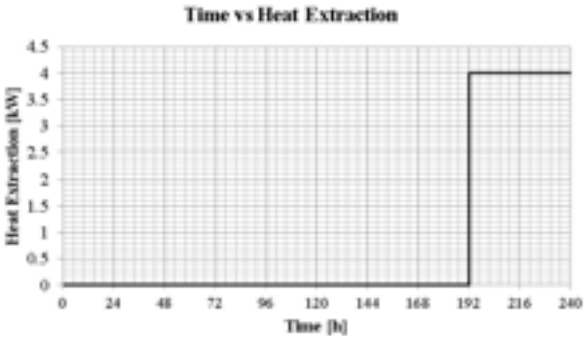

Fig. 5: Time vs Heat Extraction

All the nodes of the finite element method model started with a temperature of 20°C, the room temperature is also the same. The 10 days of simulation were divided among 1000 steps, each step represents a time of 14.4 minutes. The Autodesk Simulation Mechanical 2014 software at the end of the simulation assign a temperature for each node that compose the model. The nodes form brick, pyramidal, tetrahedral and wedges elements. Knowing the volume and density of each element can be obtained the mass. With the mass information and with mathematical models from the C_p of each material can be obtained the change in the energy stored or released.

3. Results

The solar concentrator was unavailable at the time of the A design construction, a gas furnace was built over the energy receptor. It was found that the graphite exposed at a temperature of 400°C and higher in contact with the air oxidize damaging the graphite parts until the whole part sublimates into CO_2 [17]. However, if the graphite is submerged into the heat reservoir the wear of the graphite parts use to be little to non – existent. By means of thermocouples it was found that between the energy receptor and the upper graphite disc was a temperature difference between 140°C and 200°C. This means the presence of a bottleneck to the heat flow between the aforementioned parts [1].

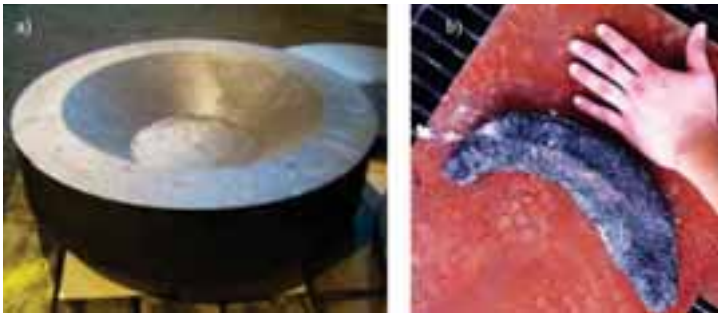

Fig. 6: Energy receptor. a) Before the charge of the TES unit b) After the charge of the TES unit.

Fig. 7: Lower graphite disc after the charge of the TES unit. a) Face of the lower disc pointing inside the crucible in direct contact with the glass melt. b) Face of the lower disc pointing outside of the crucible in contact with the atmosphere.

The TES unit was charged over a period of 6 days and 20 hours, followed this period by 9 days of cooling, with two periods of recharge of 8 hours each during the cooling stage. By using thermocouples and a data acquisition module it was possible to take and record samples of the temperature of the glass melt and the thermal insulation. The glass melt reach an average temperature between 900°C and 980°C at the end of the charge stage; the energy receptor zone reached a maximum temperature of 1200°C and the energy extraction zone reached an estimate maximum temperature of 880°C. During the charge and cooling of the TES prototype there was no device to convert the thermal energy to either mechanical or electrical energy.

Due to the aggressive degree of oxidation the following TES designs tried to diminish as much as possible the graphite parts in size and number and avoid exposing them as much as possible from the atmosphere.

The radiation reception area has a size of roughly 150 cm². In figure 9 can be seen that radiation heat losses through this area are a maximum of 72% for design B and 61% for design C from the total radiation received daily.

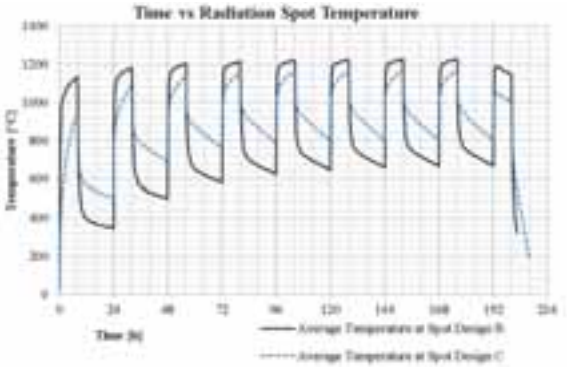

Fig. 8: Time vs Radiation Spot Temperature

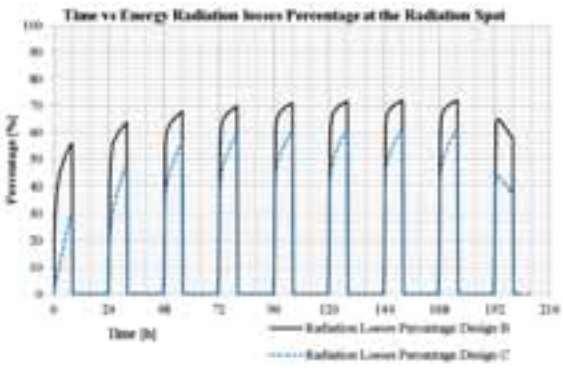

Fig. 9: Time vs Energy Radiation Losses Percentage at the Radiation Spot

The radiation losses during the charging cycle where obtained using the Eq. 5. The temperature of the central point of the energy receptor surface was taken and was assumed to be representative of the whole area. It is known that each day 45 kWh arrive at the energy receptor area. The value of 45 kWh minus the radiation losses is the energy that is stored inside the TES unit.

$$Q_{\text{Stored}} = \text{Daily Solar Energy} - \text{Radiation Losses} \quad \text{(eq. 6)}$$

With the information from the Table 3 where energy that is stored in each material is known from the finite element method analysis, the net energy can be obtained by subtracting the total energy stored at the end of the charging state minus the total energy value at the beginning of that day.

$$Q_{\text{Net Stored}} = \text{Total Energy}_{End\ of\ Charging\ cycle} - \text{Total Energy}_{Start\ of\ the\ day} \quad \text{(eq.7)}$$

The absolute energy losses by heat convection during the charging state can be obtained with the following equation.

$$Q_{\text{Convection losses, charging cycle}} = Q_{\text{Stored}} - Q_{\text{Net Stored}} \quad \text{(eq. 8)}$$

The absolute energy losses by heat convection during the rest stage can be obtained with the subtraction of total energy at the end of the rest cycle to the total energy stored at the end of the charging cycle

$$Q_{\text{Convection losses ,rest cycle}} = \text{Total Energy}_{End\ charging\ cycle} - \text{Total Energy}_{End\ rest\ cycle} \quad \text{(eq. 9)}$$

In the Figure 10 is shown the temperature in the extraction zone. If the time that the extraction zone is above 500°C is known the total energy that can be extracted from the TES unit can be obtained by multiplying the time with the heat power extracted by the Stirling Engine. The design B and C worked around 12.8 minutes and 4.2 hours respectively. The values of the total energy extracted by the Stirling Engine, the radiation and convection heat losses are shown in the summary of the Table 4.

$$Q_{\text{Extracted}} = Q_{\text{Stirlign Engine Requiered}} * t \quad \text{(eq. 10)}$$

The Table 3 shows the total amount of energy that is stored in every material that forms the TES units. The maximum and minimum temperature of each material as a sample of how uniformly the temperature is distributed is shown as well. The figures 11 and 12 are the summarized results of the finite element method for the TES design's B and C in order to facilitate the comparison of the amount of total heat stored in the designs B and C and in which materials the heat is stored. All these results will be commented in extend in the conclusion section.

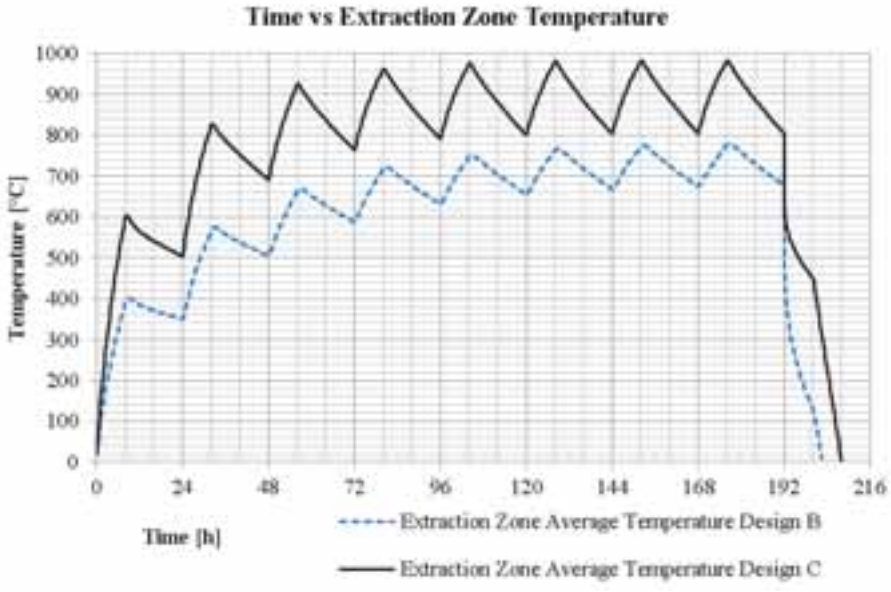

Fig. 10: Time vs Extraction Zone Temperature

Tab. 3: Stored energy in the TES units between day 8 and 9.

		Energy [kWh]		Useful Energy above 500°C [kWh]		Temp Max [°C]		Temp Min [°C]		Temp Average [°C]	
		Design B	Design C	Design B	Design C	Design B	Design C	Design B	Design C	Design B	Design C
Day 8 - Start	Graphite	8.85	11.69	2.61	5.47	674	808	662	800	673	804
	Soda lime glass	20.74	23.08	6.47	10.32	678	808	668	800	675	806
	Refractory Concrete	16.31	19.62	4.65	8.07	678	808	646	759	669	796
	Ceramic Fiber	2.85	2.93	0.13	0.32	670	799	80	46	428	499
	Metallic Container	2.18	0.69	0.00	0.00	209	121	30	52	103	76
	TOTAL	**50.93**	**58.01**	**13.85**	**24.18**						
Day 8 - End of the charging cycle	Graphite	10.28	15.48	4.96	9.27	784	1166	740	944	852	1034
	Soda lime glass	24.91	29.16	10.64	16.41	1002	1051	731	942	784	978
	Refractory Concrete	19.10	24.15	7.44	12.61	1175	1120	691	867	796	968
	Ceramic Fiber	3.24	3.56	0.32	0.66	1224	1024	82	55	500	599
	Metallic Container	2.33	0.85	0.00	0.00	209	148	30	60	111	90
	TOTAL	**59.86**	**73.21**	**23.36**	**38.94**						
Day 8 - End of the rest cycle	Graphite	7.98	11.70	2.66	5.48	678	809	666	800	677	804
	Soda lime glass	20.87	23.10	6.60	10.33	682	809	672	801	679	806
	Refractory Concrete	16.41	19.63	4.74	8.09	681	808	650	759	672	797
	Ceramic Fiber	2.87	2.93	0.14	0.32	673	799	81	46	431	499
	Metallic Container	2.20	0.69	0.00	0.00	211	121	30	52	104	76
	TOTAL	**50.34**	**58.05**	**14.14**	**24.21**						
Day 9 – Until energy extraction zone cool down	Graphite	7.98	10.46	2.66	4.24	678	1026	481	500	714	802
	Soda lime glass	20.60	20.58	6.33	7.82	815	874	549	565	674	728
	Refractory Concrete	16.31	18.10	4.65	6.55	966	962	538	557	670	717
	Ceramic Fiber	2.87	2.64	0.14	0.21	1051	861	81	43	434	451
	Metallic Container	2.20	0.60	0.00	0.00	210	115	30	49	104	68
	TOTAL	**49.96**	**52.39**	**13.77**	**18.82**						

Tab. 4: Energy gain and losses of the TES units design B and C

Summary	Design B	Design C
Radiation losses during charging stage [kWh]	30.79	24.57
Net energy stored during charging stage [kWh]	14.21	20.43
Energy stored at the end of the charging stage [kWh]	8.93	15.20
Heat losses by convection during charging stage [kWh]	5.28	5.24
Heat losses by convection during rest stage [kWh]	9.53	15.16
Total energy extracted by Stirling engine [kWh]	0.85	16.80
Useful energy remained in the TES unit [kWh]	13.77	18.82

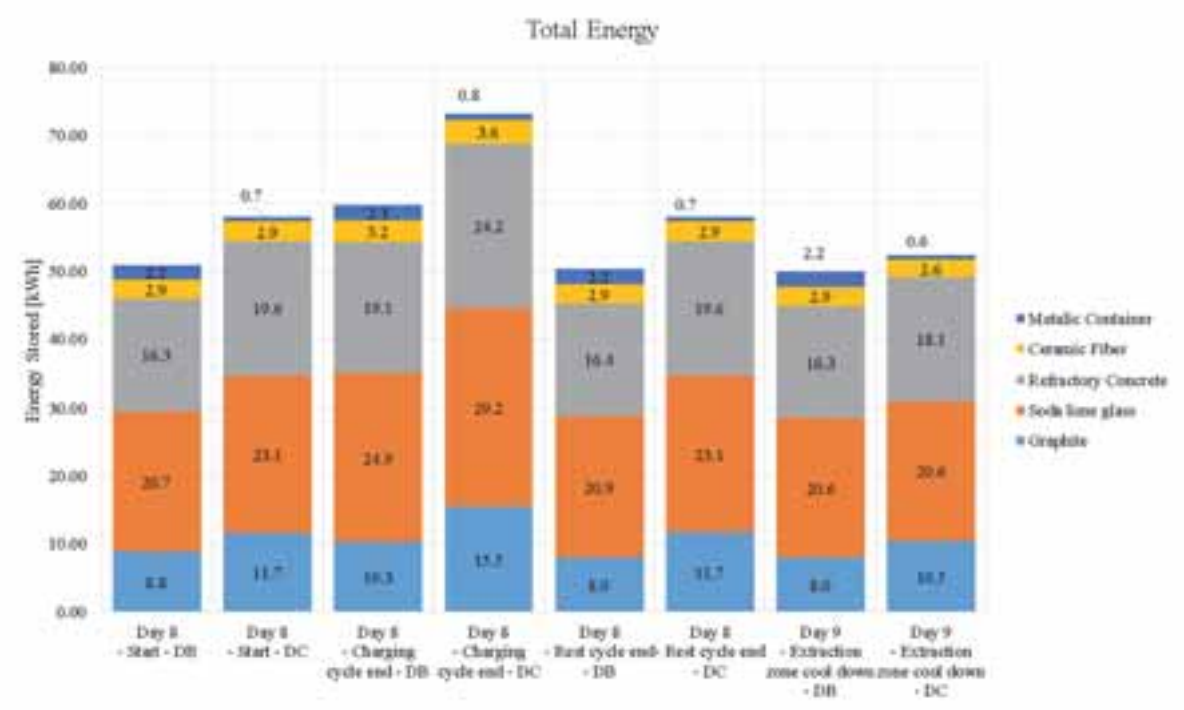

Fig. 11: Total energy stored by material between days 8 and 9 designs B and C.

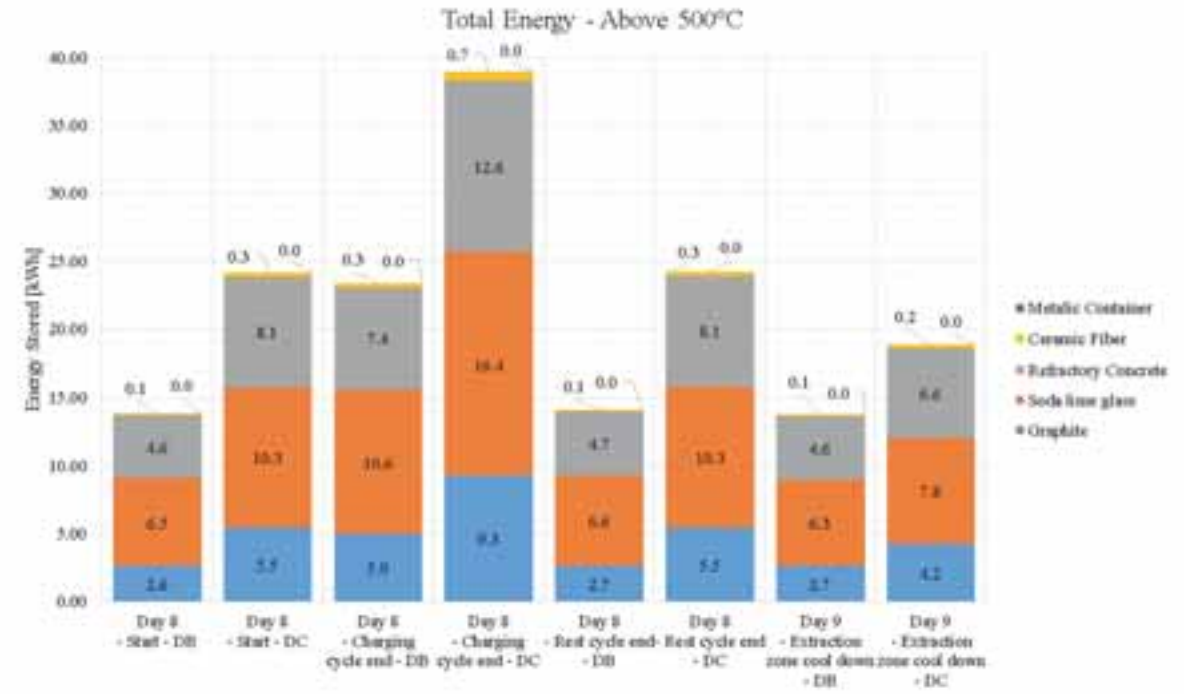

Fig. 12: Total energy above 500°C by material between days 8 and 9 designs B and C.

For the Design B four control points where taken to get an idea about the inside temperature of the reservoir heat body. Point a) and d) were taken because along the simulation they shown the highest and lowest temperature points respectively during the charging cycles. Point b) shown the highest temperature during the rest cycles, during the rest cycles point a) took the lowest temperature values. Point c) shown the lowest temperature values during the energy extraction stage.

For the Design C five control points where taken. Point a) and e) were taken because along the simulation they shown the highest and lowest temperature points respectively during the charging cycles. Point d) and b) shown the highest and lowest temperature during the rest cycles. Point c) shown the lowest temperature values during the energy extraction stage. In the figure 13b all control points are slightly off center of the model cut, just point b) is near the periphery of the crucible base normal to the TES unit cut.
This analysis consist in take the highest and lowest temperature values of the heat reservoir, any other point should lie between these two values. This should be a good approximation of the temperature of the heat reservoir and how well the heat flows through it.

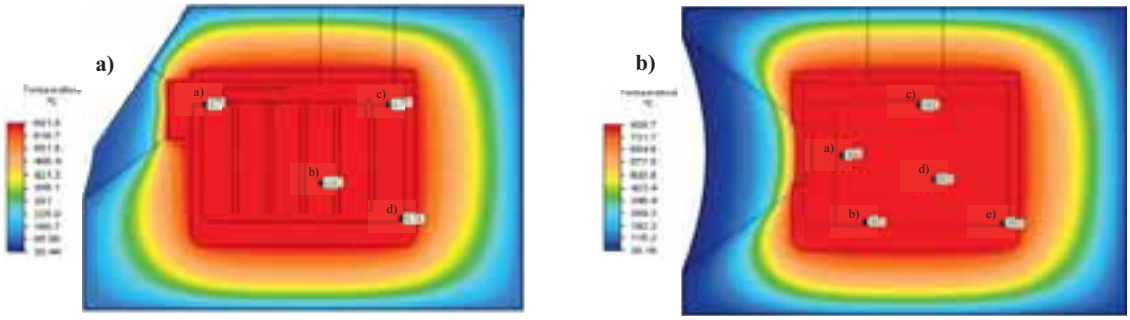

Fig. 13: Heat reservoir temperatures at the beginning of the day 9. a) Design B, b) Design C

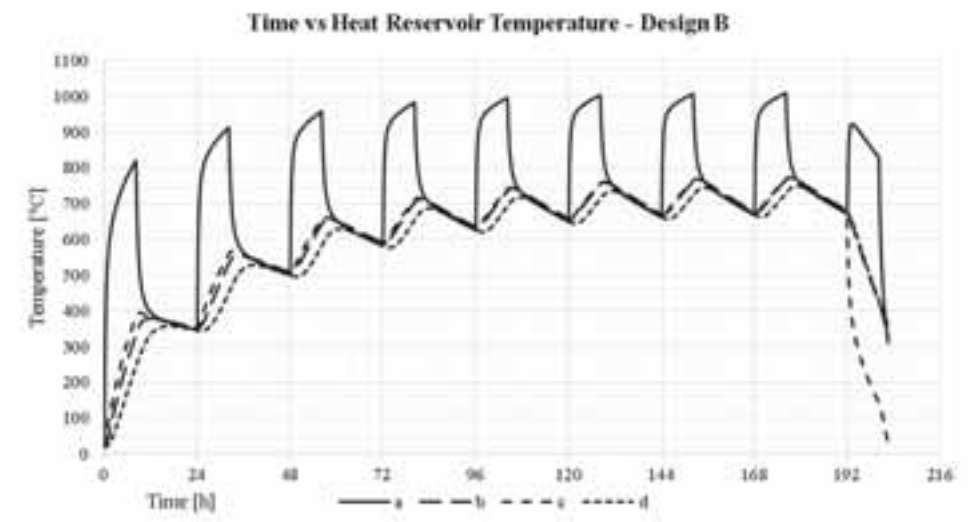

Fig. 14: Time vs Heat Reservoir Temperature - Design B

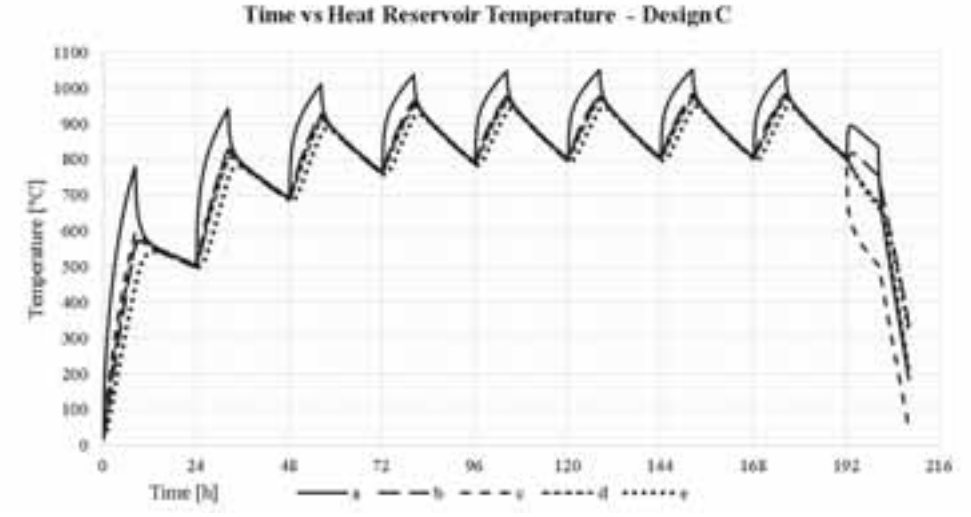

Fig. 15: Time vs Heat Reservoir Temperature - Design C

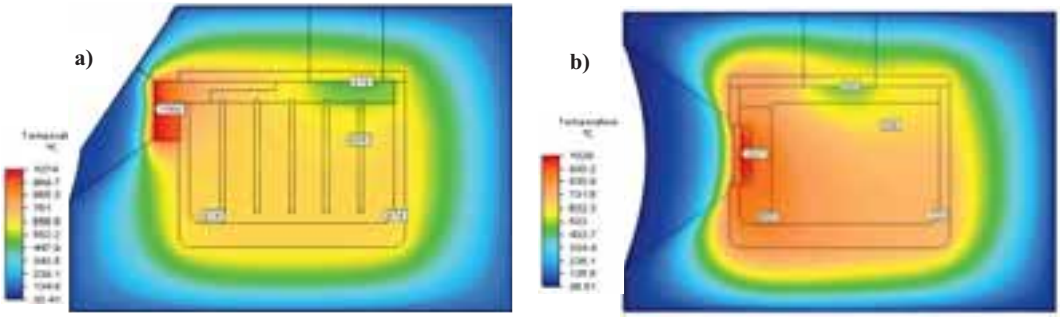

Fig. 16: Temperatures inside the TES unit at the beginning of the day 9 a) Design B after 14 minutes. b) Design C after 4.2 hours.

4. Conclusions

After many days of charging the TES units they reach a cyclical behavior, no matter how many days the system charges. The TES units shown can be consider charged after the day 4 or 5. Any gain in energy from more charge cycles are negligible (Figures 14 and 15).

The energy exchanged between the ambient and the energy receptor represent radiation heat losses from 60% to 70% of the total energy received daily. The design of a radiation cavity is a must to reduce the radiation losses. The view factor from the receptor to the environment was omitted in the equation 5 in order to get a better understanding of the radiation heat losses at their full potential, thus promoting attention to a meticulous research of the design of a radiation cavity in the near future and supporting the idea of adding an additional component to a system that tries to be has simple has possible.

The total amount of heat stored available to conversion in the TES units shown in the Figure 11 is reduced to the values shown in the Figure 12 because it must be above the working temperature of the conversion engine. For the present designs, must be above 500°C.

The design B and C both had useful energy above the 500°C after the extraction zone reached a temperature below the Stirling Engine working temperature, however the thermal conductivity of the soda lime glass is not good enough to transport the useful energy above 500°C along all its mass to the extraction point at the required heat rate.

Increase the temperature of the heat reservoir can enhance the thermal conductivity value of the glass dramatically (Fig 3) in order to increase the heat extraction rate and as a side effect improve the performance of the heat input.

Augment the area of heat extraction can uniformly consume the energy of the heat reservoir body delaying the event of reaching at the energy extraction zone a temperature below the working temperature of the conversion engine.

Shorten the length dimensions in the heat reservoir can improve the speed at which the heat spread uniformly through the heat reservoir.

In the ideal case as the heat flow cross a body mass the temperature should change homogeneously in every point of its lump in a short time, in reality this is not the case. Design C has a better spread of the heat across its heat reservoir body during the charging and rest cycles than the Design B as shown in figures 14 and 15. The sample point in both figures represent the highest and lowest temperature values inside the lump of the glass heat reservoir. In the case of the Design C the graphic lines are closer than those of the Design B. Once the TES units have achieved a cyclical behavior the maximum difference of temperature at the end of the charging cycle of the day 8 are 279°C and 110°C for the designs B and C respectively. A reason why the Design C has a better heat flow through its heat reservoir is that the energy receptor zone is slightly inside the heat reservoir container and is communicated to the inside of the TES unit through a bigger area than in the case of the Design B.
The removal of the bottlenecks between the energy receptor and heat reservoir have a great impact in the performance of the TES unit. Besides the heat flow bottle neck present in the TES unit B design, absent in the TES unit C, the graphite conductor plates in the unit B are perpendicular to the heat flow instead of being in

the same direction as in the TES unit C providing an easier path to the heat flow and increasing the amount of heat being stored inside the TES unit in this last design. The previous reasons explain why the TES unit C store more heat than the unit B.

Once the heat extraction stage begins has seen in the figures 14 and 15 the graph lines of the Design C are closer than those in the Design B. The heat flow through the heat reservoir of the Design C is more efficiently compared to the Design B. As the TES unit C store more heat, higher temperatures are achieved in the glass heat reservoir, this means that the overall glass lump thermal conductivity values will be higher in the TES unit C compared with the unit B. Once both TES units achieve a cycle behavior the glass inside the TES unit B has thermal conductivity values between 6.36 w/m-°C and 10.61 w/m-°C, meanwhile the TES unit C has thermal conductivity values between 12.92 w/m-°C and 28.30 w/m-°C. In the rest stages in designs B and C the temperature tend to homogenize uniformly in a relative short time (Figures 13, 14, 15).

The alumina crucible store a similar amount of energy compared to the main heat reservoir of soda lime glass, however the alumina has a poor thermal conduction value, so extract this energy from the crucible at the desired output power may not by viable.

The combined energy losses by radiation and by convection during the charging stage almost equals the convection heat losses during the rest stage once the system has achieve a cyclical behavior.

Even if the designed TES unit keep using graphite for the receptor and extraction heat system the number and size of these parts have diminished. To protect the graphite from the oxidation at high temperatures in the presence of air strategies like surrounding the graphite parts with an inert atmosphere or covering them with a coating of silica, silicon or silicon carbide are available[15, 16]. The designs B and C keep their graphite parts as close to the core of each design in order to avoid as much as possible the contact of the graphite parts with the atmosphere. The Design C fulfill the aforementioned requirement better than the Design B.

In a general way the TES unit B has a lower performance than the unit C due to physical flaws in its design that hinders the amount of heat rate that can be directed into the core of the TES unit B.

Work on the development of a TES unit that can work 24 hours uninterruptedly is in advance as well as new experimental tests. The research group is currently working on the design of radiation cavity to minimize the radiation heat losses and in a phase change material system to be installed on the original energy extraction zone to be in contact with the full upper area to enhance the energy extraction zone in order to extract as much a useful energy as possible before this area reach a temperature below the working temperature of the engine device.

5. Acknowledgments

The authors acknowledge Institute of Renewable Energy (IER-UNAM) through the Mexican Center of Innovation in Solar Energy (CeMIE-Sol) (Strategic Project 05 "Development of solar thermal storage tanks"), through which it was possible to develop research and support the training of human resources at postgraduate level.

6. References

[1] Cárdenas, B. 2014. Tanque de Almacenamiento de Energía Térmica. Instituto Tecnológico y de Estudios Superiores de Monterrey, Nuevo León, México.

[2] Trombe, F., & Le, A. 1973. Thousand kW solar furnace, built by the National Center of Scientific Research, in Odeillo (France). Solar Energy, 15(1), 57-61.

[3] Kronhardt, V. Alexopoulos, S. Reissel, M. Sattler, J. Hooschmidt, B. Hänel, M. Doerbeck T. High-temperature Thermal Storage System for Solar Tower Power Plants with Open-volumetric Air Receiver Simulation and Energy Balancing of a Discretized Model. Energy Procedia, 2014.

[4] Amador, B. 2012. Materiales de cambio de fase para almacenamiento de energía solar. Instituto Tecnológico y de Estudios Superiores de Monterrey, Nuevo León, México.

[5] Garcia, L. 2010. Tanque Solar de Alta Temperatura. Instituto Tecnológico y de Estudios Superiores de Monterrey, Nuevo León, México.

[6] Gutiérrez R. 2014. Diseño y Simulación de Tanque de Almacenamiento Térmico Solar. Instituto Tecnológico y de Estudios Superiores de Monterrey, Nuevo León, México.

[7] Shelby, J 2005. Introduction to glass science and technology. (2nd Ed). Cambridge: Royal Society of Chemistry.

[8] Rasor N.S, McClelland J.D. Properties of graphite, molybdenum tantalum to their destruction temperatures. Journal of Physics and Chemistry of Solids 1960; 15: 17-26.

[9] Kovacec M, Polipovic A, Stefanic N. Impact of glass cullet on the consumption of energy and environment in the production of glass packaging material. Recent Researches in Chemistry, Biology, Environment and Culture. Monteux, Switzerland, 2011.

[10] Comprit 180H M. http://www.energiaencontrol.com/ Accessed 16- September -2014

[11] Thermal Ceramics Kao-Tab 95 High Alumina Castables. http://www.matweb.com/ Accessed 16-September -2014

[12] SuperMag 1200 Spun Soluble Blanket. http://www.nutec.com/supermag1200 Accessed 9-September -2014

[13] ASTM A36 (SS400, S275) Structural Carbon Steel. http://www.makeitfrom.com/material-properties/ASTM-A36-SS400-S275-Structural-Carbon-Steel/ Accessed 28-September-2015

[14] Cengel, Y. 2011. Heat and mass transfer: Fundamentals and applications (3rd Ed.). Singapur: McGraw-Hill.

[15] Trinuruk, P., & Obara, T. 2013. Concept of prismatic high temperature gas-cooled reactor with SiC coating on graphite structures. Annals of Nuclear Energy.

[16] Zhi-qiang, F., Cheng-biao, W., Chun-he, T., Hong-sheng, Z., & Jean-Charles, R. 2013. Oxidation behaviors of SiO2/SiC coated matrix graphite of high temperature gas-cooled reactor fuel element. Nuclear Engineering and Design.

[17] Guo, W., & Xiao, H. 2007. Modeling of TG curves of isothermal oxidation of graphite. Material Science & Engineering A, 197 – 200